Study of a Fluid-Controlled Solid Rocket Motor for a Mars Orbiter

NORMAN S. COHEN* AND KENNETH R. SMALL†
Lockheed Propulsion Company, Redlands, Calif.

Fluid-controlled solid rocket motors are characterized for a specified Mars mission in the 1973 to 1975 time period. Designs are constructed for 2400-lb and 5000-lb vehicles, with acceleration level as a parameter. The engine is to perform midcourse correction, Martian orbit insertion, and orbit trim maneuvers. Mission specification, results of tradeoff analyses, and performance and operational features are summarized. Important design factors include interior ballistics with an eroding nozzle throat, impulse bit capability, and thermal control (mission life) with ClF_5, F_2, or OF_2 used as an injectant to provide ignition, thrust level control and (by shutting if off) thrust termination. Designs incorporate a spherical solid rocket motor containing a suitably tailored solid propellant. Spherical tanks for the liquid and for helium pressurant are mounted forward. Optimum engines operate at approximately constant thrust, 3-g burnout, with appropriate feedback signals producing cut-offs per demand ΔV increments. The feed system includes pressure regulators, explosive valve banks (serving isolation and flow control functions), a liquid surface tension device, plumbing and injectors. A flexible (Lockseal) nozzle provides thrust vector control. The baseline liquid is ClF_5, and F_2 is the preferred advanced liquid. Performance growth also is available via the solid propellant.

Introduction

AN earlier paper[1] described the principles of operation, results of early tests, and preliminary design evaluation of a fluid-controlled solid rocket motor. Basically, all combustion exhibits pressure threshold levels, and a rocket motor can be designed so that mass generation from the solid is incapable of self-sustaining any pressure except the ambient back pressure. Then a fluid can be added to make up the mass deficiency for burning at a given P_c. This fluid can fulfill the multiple roles of ignition, thrust level control, and termination. It is not a principal function of the fluid to provide chemical stoichiometry, although certain fluid-solid combinations will indeed augment the performance of the solid. As a result, the fluid/solid ratio (F/S range) of interest is 0.2 to 1.0, and there is freedom of choice in fluid type and F/S within this range. Particular selections are subject to a number of considerations and particular application requirements. Prior studies have shown the economic attractiveness of such systems.[2]

The present study was done to characterize fluid-controlled solid propulsion systems for a specific Mars transit and orbital mission contemplated for 1973 and 1975. Results are to be used by NASA for continued evaluation of the fluid-controlled solid for this and other projected space missions. (For additional information, the interested reader is referred to Ref. 3.) The mission requirements are summarized in Table 1, and propulsion system envelope configurations are illustrated in Fig. 1. The passive transit orientation is nozzle-to-sun. The spacecraft vehicle weight is the weight launched onto the transit trajectory to Mars. It is contemplated that a 2400-lb vehicle will be launched by a Titan IIIC booster system, and a 5000-lb vehicle by a Titan IIIF-Centaur booster system. Prelaunch transportation and handling requirements and characteristics of the launch environment were obtained from the Titan IIIC manual.

Propulsion system designs included the following guidelines: the payload will be passively thermally conditioned to 70°F; there will be no venting to space of pressurant, oxidizer, or hydraulic fluid; state-of-the-art technology will be consistent with a 1971 cut-off date for a 1973 mission; power will be available from the payload except for unusual requirements such as heat exchangers, electrically-driven thrust vector control (TVC) or pumps, etc.; an existing suitable solid

Table 1 Propulsion requirements to orbit Mars in 8 months

Midcourse firings	0 to 3 (max)
Total accumulated ΔV	10 m/sec (max)
Minimum ΔV pulse	1.0 m/sec
Accuracy of minimum pulse	± 0.1 m/sec, 3σ
Occurrence	
Injection corrections	at launch +1 to +10 days
Approach corrections	at encounter −10 to −1 day
Orbit insertion firing	1
Total ΔV	1640 m/sec
Occurrence	at encounter
Orbit trim firings	3 to 6 (max)
Total accumulated ΔV	150 m/sec
Minimum ΔV pulse	1.0 m/sec
Accuracy of minimum pulse	± 0.1 m/sec, 3σ
Occurrence	
First trim	encounter +1 day
Last trim	encounter +6 months
Thrust vector control	
Omnidirectional angle	3 deg
Response	10 cps

Presented as Paper 69-446 at the AIAA 5th Propulsion Joint Specialist Conference, U.S. Air Force Academy, Colo., June 9–13, 1969; submitted June 4, 1969; revision received October 3, 1969. This work was sponsored by the NASA, Office of Advanced Research and Technology, under Contract NAS 7-701. Technical monitoring was provided by the Jet Propulsion Laboratory. The authors acknowledge the contributions to this program of G. Mills and D. E. Taylor of Lockheed Propulsion Company, and R. Neff of the Lockheed Missiles & Space Company. J. Behm and W. Dowler of the Jet Propulsion Laboratories provided guidance to the program for the NASA.

* Supervisor, Combustion Section, Engineering Research Department, Program Manager. Associate AIAA.

† Senior Design Engineer, Engineering Research Department, Project Engineer. Associate AIAA.

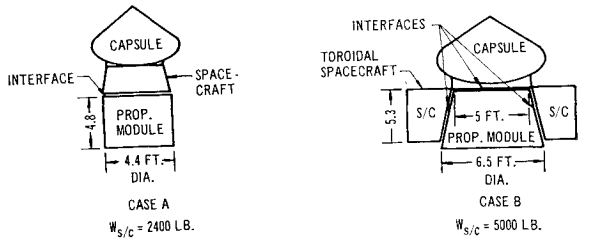

Fig. 1 Propulsion system envelopes and spacecraft configurations.

propellant will be used; for the liquid oxidizer, ClF_5 will represent the "Earth-storable" class, and OF_2 and F_2 will represent advanced "space-storable" liquids; the maximum F/S will be 0.5, based on existing small-scale delivered performance data, but may be optimized based on projected full-scale delivered performance in the context of growth potential; acceleration level will be optimized within the constraint of a 5-Earth-g maximum.

Systems Definition

Required propellant weight (total impulse) for each of the two vehicle weights is determined as a function of propulsion system mass fraction and delivered specific impulse (I_{sp}) from the well-known ΔV equation. Estimates for initial sizing were obtained from previous studies. Criteria that provided the basis for selection of the solid propellant included specific impulse with the specified liquid injectants; processibility, mechanical properties, safety, and space-storability; density; burning rate and tailorability; burn rate pressure exponent, temperature sensitivity, and deflagration pressure limit; hypergolic ignitability; flame temperature and corrosivity of combustion products; availability confidence, and firing experience. In the choice between F_2 or OF_2 as the advanced liquid oxidizer, F_2 was selected chiefly because of higher I_{sp}, lower corrosivity of combustion products bearing upon nozzle erosion and insulation requirements, and essentially equivalent space-storability in that the particular characteristics of this mission did not take advantage of the better thermal properties of OF_2.

Modes of Operation

A tradeoff was performed between a constant-acceleration mode and a constant-thrust mode of impulse delivery for orbit insertion. Principal advantages of the former include a shorter burn time for a given burnout acceleration level (Fig. 2), and the feasibility of eliminating pressure regulators. The disadvantages include a higher maximum pressure and either active flow modulation to maintain adequate injector ΔP (efficiency and feed system stability) or a still higher initial tank pressure. It was determined that the pressure-sensitive weight differences were more significant than the burn-time sensitive weight differences, and it was judged that the pressure regulators would be less complex and more reliable than a throttling system. Consequently, a nominally constant thrust mode was selected.

Operating pressure for each thrust level is established by fluid-controlled solid interior ballistics characteristics.[1] With burning rate directly proportional to pressure, selection of a fluid/solid ratio dictates the ratio of solid-propellant burning surface area to nozzle throat area (motor K_n). The burning surface area is established by solid rocket design considerations and, with the resulting throat area, the requisite pressure is achieved by the proper liquid injection rate. The nozzle throat area establishes nozzle size for a given expansion ratio, and influences TVC requirements. Nozzle erosion introduces a minor complication, as will be discussed subsequently.

For corrections, use of the main thruster to provide a minimum impulse bit (MIB) as little as 0.05% of its total impulse capability is a cost-effective approach if it can be accomplished. Alternatives include throttling the injection rate as much as reliable hypergolic ignitability in vacuum will allow, or use of auxiliary hybrid thrusters, each of which requires additional components. Required total impulses for MIB's are given by $I_{bit} \simeq 0.105\ W$, where W is vehicle weight. Because ~95% of the propellant is used for orbit insertion, impulse bits can be characterized by just two values of L^*; initial L^* for midcourse correction, and post-insertion L^* for orbit trims. For impulse-bit analysis, a transient ballistics computer program has been written which accounts for the valve open and close functions, empirical ignition delay data, variable injector ΔP and characteristic velocity c^*, and F/S imbalances. Preliminary calculations established the feasibility of delivering MIB at design injection rates, although the orbit trim pulses would be completely transient. The auxiliary thruster approach was dismissed, but provision for a dual injector was retained subject to analysis of MIB error with the single injector. Some form of ballistics feedback control would be used to generate the valve close command.

With respect to TVC (thrust vector control) requirements, factors considered included vehicle control frequency and angular rate requirements; center-of-gravity shifts due to propellant motion and expenditure; propulsion module position, launch transient, lateral velocity, and pointing errors; attitude cycling to maintain autopilot activity; duty cycle analysis, and TVC system selection factors. The analysis revealed probable worst-case requirements to be at 5 g thrusting and to consist of ~2° of deflection with an angular response rate of 8 cps; these are within specifications, so the detailed design could adhere to the specifications.

TVC systems evaluated included the Lockseal (flexible seal, movable) nozzle, liquid injection, and jet vanes. The Lockseal system was selected on the basis of weight, operational simplicity, operational flexibility, and predictability. Of particular concern with the other systems was MIB directional capability when a significant part of the thrusting is in a transient mode. On the other hand, the Lockseal nozzle is precisely pointed. Also, the ability of a reactive fluid to produce chemically-augmented side impulse is unlikely because of the lack of fuel value of the fluid-controlled solid exhaust. The LITVC was much heavier, even with reactivity assumed, because of the possible need to maintain the requisite angle for the full duration.

Propulsion System Configurations

Solid rocket motor designs considered were spherical chambers employing combined conical/cylindrical grain designs and low-L/D cylindrical chambers employing either internal-burning or end-burning grain designs. The spherical solid rocket motor was selected essentially on the basis of payload capability. Spherical motors are state-of-the-art for space applications.

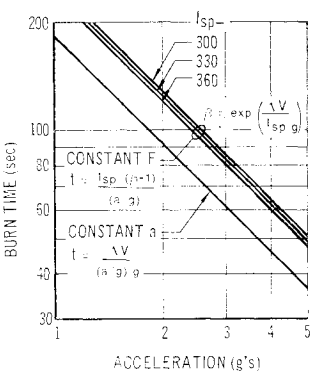

Fig. 2 Burn times for various thrusting modes; either spacecraft size.

For the liquid system, various pump-fed systems proved to be unattractive on a weight basis because a convenient means of providing motive power which would exist in a biliquid or hydrazine-controlled solid engine is not available. On the other hand, the relatively small liquid volume as compared to a biliquid or conventional hybrid (liquid/solid ratio >3) engine favors the use of inert gas pressurization. Helium pressurization also has the advantage of simplicity, particularly with fluorinated liquid.

All tanks are spherical for minimum weight. The initial major consideration was envelope compatibility, which favored positioning the solid rocket motor forward and the liquid system as a cluster of tanks (two liquid, two pressurant) around the rocket nozzle. Environmental thermodynamics, however, necessitated positioning the liquid system forward of the solid rocket motor and is discussed subsequently. This resulted in envelope length violations to achieve optimal nozzle expansion ratio. Abundant room is available for packaging control components.

Several component commonality approaches were evaluated to reduce costs of changing propulsion system size or propellant type. For each liquid, it was determined that by using a single liquid tank for the smaller vehicle, two of these tanks could be used for the larger vehicle at only a slight performance penalty. Interliquid tank commonality also was considered, wherein the single fluorine tank entailed less payload penalty to the ClF_5 system than vice-versa. However, this payload penalty to the ClF_5 system is significant and, considering the cost of building a tank capable of prelaunch liquid nitrogen subcooling that would not be employed with ClF_5, interliquid commonality did not appear to offer a worthwhile saving. The approach of using an offloaded large solid motor for the small engine was unsatisfactory because it would degrade payload capability by ~20%, markedly increase L^* (poor response), and require changes in the injectors, nozzles, and liquid system. Clustering of two small engines for the large vehicle was dismissed from the standpoints of vehicle dynamical uncertainties and more complex control requirements. Finally, it was determined that performance uprating by loading a suitable advanced solid propellant without further system changes would be attractive and feasible.

Transit and Orbital Thermodynamics Study

A mission thermodynamics study conducted by Lockheed Missiles & Space Company as a separate task had a significant impact upon the design study.[3] The objective was to establish the thermal feasibility of the several initial design configurations with the three liquids, and minimum weight parameters of feasible systems. Storage of ClF_5 was feasible for each of the sizes and forward packaging configurations considered. However, a sunshield is required for the large vehicle, owing to the toroidal payload configuration, to maintain the ClF_5 close to the payload temperature and avoid overpressure. With the forward payload design of the small vehicle, the sunshield is not required because the tank can radiate to space, but tank insulation is needed to prevent freezing in transit.

Neither F_2 nor OF_2 is feasible in the large vehicle because of the toroidal payload, which provides a high boundary temperature and prevents radiation to space. The effect of moving the payload forward as in the small vehicle could, in part, be evaluated by examining the results for the small vehicle. In that system, both cryogens successfully arrived in Martian orbit with the assistance of an insulated sunshield. Insulating the sunshield permits less insulation on the tanks so that the heat absorbed by the liquid internally from attached structure can be more easily radiated to space. Insulation thicknesses were optimized for minimum system weight.

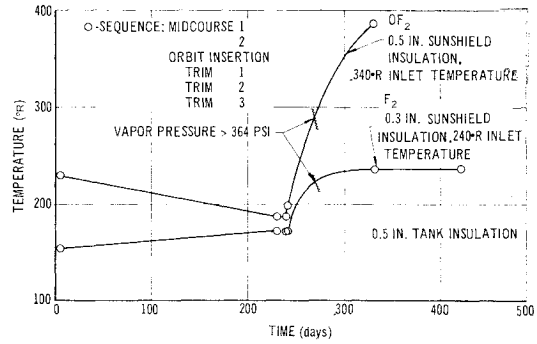

Fig. 3 Temperature histories of F_2 and OF_2 liquids over the mission profile.

Following Martian orbit insertion, radiation heating due to the close proximity of the planet was found to be significant for OF_2 and F_2. At this point in the mission, very little liquid remains; this contrasts with the full tanks considered in previous NASA studies wherein the effect of planetary radiation heating is negligible. The system is now "boxed in" because any additional shielding or insulation to combat thermal heating from both sun and Mars will prevent radiation to space of the internal heating absorbed throughout the mission. Although heating from the liquid line was minimized by positioning the valve so that the line is evacuated for half its length, strut-support heat leaks were significant. The optimum set of parameters produced a 30-day lifetime in Martian orbit.

Any apparent thermodynamic properties advantage of OF_2 relative to F_2 was of little consequence. Examination of a number of temperature histories, e.g., Fig. 3, indicated that vapor pressure buildups (no venting allowed) were of the order of a day apart between the two liquids. Consequently, the two liquids are of comparable feasibility or infeasibility, so that F_2 is preferred on the basis of higher I_{sp} and much reduced combustion products corrosivity.

Analysis variations to improve the feasibility of 6-month orbit duration were not performed, but the following qualitative decisions were made for the detailed designs: 1) use of a single liquid tank in the small vehicle (also good for size commonality) and acceptance of envelope penalty, 2) reduction of internal heating through methods such as tension-type supports or decoupling mechanisms (with or without Mars shielding), 3) removal of the heat exchanger for the helium pressurant and acceptance of the weight penalty of very cold gas and 4) recommendation of a forward payload for the large vehicle with F_2, but any resulting lateral volume would not be considered available for propulsion.

Postburn nozzle cooldown did not have a significant effect upon the oxidizer heating and the motor temperature remained within allowable limits. With a sun-oriented nozzle, the solid-propellant temperature reached an acceptable minimum of −35°F. The solid-propellant ballistics design for orbit insertion employed the burning rate at this temperature; however, the sensitivity of burning rate is 0.1%/°F for the propellant selected, so design temperature errors or off-design temperature operation for impulse-bit thrusting are of little consequence.

Detailed Design

Beginning with existing subscale data, delivered performance in full scale was estimated by individual analysis of sources of performance loss: incomplete combustion, chamber heat loss and insulation ablation, nozzle divergence loss, nozzle heat and friction losses, nozzle submergence loss, and two-phase and nonequilibrium nozzle flow losses. The analysis was assisted by reference to applicable liquid, solid, and conventional hybrid information. An optimum nozzle

Table 2 Propulsion system weights

	2400-lb vehicle (ClF_5)			2400-lb vehicle (LF_2)			5000-lb vehicle (ClF_5)			5000-lb vehicle (LF_2)		
Maximum g-level	1	3	5	1	3	5	1	3	5	1	3	5
a) Total inert weight	288.10	262.85	284.62	296.74	274.89	296.28	532.04	501.98	587.52	554.20	533.09	619.57
b) Propellant weight expended	1096.1	1096.1	1096.1	1024.6	1024.6	1024.6	2290.0	2290.0	2290.0	2147.0	2147.0	2147.0
c) Propellant residuals	20.99	20.99	20.99	19.25	19.25	19.25	45.08	45.08	45.08	42.15	42.15	42.15
d) Insulation and nozzle material expended	58.66	56.29	47.43	55.47	53.54	45.02	111.71	101.97	84.97	107.73	98.38	81.85
Initial mass fraction $= \frac{b}{a+b+c}$	0.781	0.795	0.783	0.765	0.778	0.766	0.800	0.808	0.797	0.784	0.790	0.766
Burnout mass fraction $= \frac{b+d}{a+b+c}$	0.822	0.835	0.816	0.806	0.818	0.798	0.838	0.843	0.813	0.822	0.825	0.794
Propulsion system weight	1405.2	1379.9	1401.7	1340.6	1318.7	1340.1	2867.1	2837.1	2922.6	2743.3	2722.2	2808.7

expansion ratio based on delivered performance and preliminary weight analyses was determined as approximately 54.

Fluid/solid ratio was optimized for maximum payload fraction by generating equations for delivered performance and mass fraction as a function of F/S. Earlier parametric study results assisted in this evaluation.[4] Optimum values of F/S were 0.71 for ClF_5 and 0.73 for F_2, with the selected solid propellant. Therefore, the designs could proceed at the ground rule maximum of 0.50, and any benefits of the higher values would be considered as growth potential subject to demonstration in full scale. Because of tank size commonality, the 5000-lb vehicle engines operate at $F/S = 0.47$. Total propulsion system package weights vs maximum g-level are shown in Table 2.

Solid Rocket Motor

Nozzle erosion as a function of design thrust level was analyzed in detail for the subject designs using existing thermochemical techniques. (The theory was evaluated by comparison with data for conventional hybrid engines from tests of reasonable representative thermochemistry and duration.) The results in Fig. 4 for thrust corresponding to 3-g burnout acceleration show that erosion is comparatively severe with OF_2 injection.

Nozzle erosion in a solid rocket causes reductions in chamber pressure and thrust which, in a space application, is not important as long as it is provided for in thermal and structural design. However, with a fluid-controlled solid, nozzle erosion causes an F/S excursion with attendant performance and utilization penalties. The instantaneous F/S is dictated by the solid rocket motor K_n and is independent of fluid injection rate. With a neutral (constant burning surface area) grain design, erosion reduces K_n and increases F/S. The obvious solution to this problem is tailoring the basic grain design for the requisite progressivity (increasing burning surface area) to match the nozzle throat erosion function. Therefore, K_n and F/S remain constant. The spherical "conicyl" grain design selected is amenable to a wide range of burning surface area functions (regressivity-neutrality-progressivity). Progressive functions could be generated by tailoring the shape of the inhibited area in the proximity of the nozzle.

Many configurations were characterized during this study, and a design precisely matching the erosion function of Fig. 4 for ClF_5 and F_2 was established. During actual development, the precise configuration of the tailoring zone would be established by test results. The progressivity called for in the case of OF_2 would have required a more radical change in solid rocket motor design, reducing mass fraction potential, and its magnitude is such as to more seriously affect nozzle weight and consequences of variability.

Fluid-controlled solid ballistics with an eroding throat and matching progressive grain were characterized. Pressure P_c decreases and thrust F increases with time, the total variations being about 10% at 3 g (Fig. 5). To meet specified burnout acceleration levels, the initial pressures were recalculated for requisite lower values as compared to those for a neutral grain with no erosion. Liquid injection rates are set accordingly and will vary passively in the course of the burn duration in accord with the ballistics equations of the fluid-controlled solid to maintain constant F/S. No active modulation is required. The net effect, compared with a neutral grain and no erosion, is a slight reduction in average thrust and a slight increase in burn duration.

The spherical combustion chamber shell is selected because of a) a superior resistance to deformation, an important consideration because resistance to manufacture and handling abuse proved controlling in some designs, b) a geometric stress and weight advantage when criteria other than handling loads are controlling, c) attractive grain volumetric loading and web fraction potential within the constraints of pressure vs burn time requirements, grain design progressivity required and nozzle length minimization, d) attractive injector distribution for good combustion efficiency, and e) minimum exposed surface area requiring insulation when meeting other constraints. A low-silicon stainless steel is used in all designs to provide generic similarity between all tankage

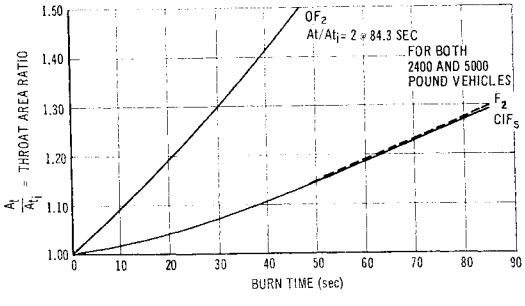

Fig. 4 Nozzle erosion curves.

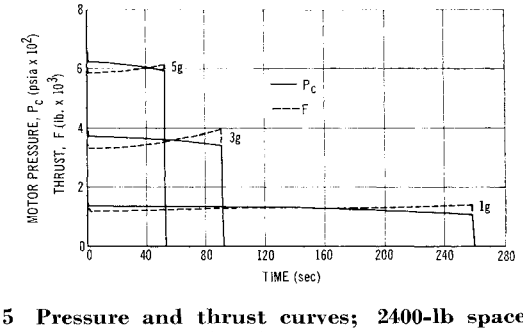

Fig. 5 Pressure and thrust curves; 2400-lb spacecraft, ClF_5 liquid.

materials and fabrication processes and thereby to improve reliability and reduce cost. This material can be shear-spun or hydroformed to an undersized hemispherical shape, trimmed for bosses and mounts, then welded before cryogenic stretch-forming as in the Ardeform process. It has superior strength and toughness at room and cryogenic temperatures, high weld efficiency, and is compatible with fluorinated liquids.

Chamber insulation and burn surface inhibitors are composed of magnesium fluoride-filled, buna-N rubber. This material was optimal with respect to the following criteria: ablation rate in the encountered combustion environment, thermal diffusivity and heat of ablation, mechanical properties, and bondability. Required thickness was established by heat transfer and thermochemical analysis.

A submerged ablative nozzle with a high density graphite throat is used in all designs. The aerodynamically contoured entry and expansion cone are composed of tape-wrapped, carbon-fiber-reinforced phenolic. Asbestos-fiber-reinforced phenolic serves as additional throat backup insulation to protect the titanium alloy structural backbone. A reinforced elastomer design provides the flexible seal.

Liquid System

Ardeform 301 stainless steel spherical tanks also are employed here for reasons summarized in the previous section. For expulsion control, a surface tension device that functions as a capillary propellant management system in a zero-g environment was selected over competitive systems chiefly because of its low weight and passive simplicity. It is also superior with respect to design and manufacturing simplicity, absence of vapor in the effluent, insensitivity to dynamic loads, unlimited cycle capability (simple system check-out), and expulsion efficiency.

Liquid orientation during thrusting is maintained by the acceleration force. In recognition of TVC and orbit-trim impulse-bit requirements, series expulsion was used from the two tanks associated with the large vehicle to avoid the possibility of two-phase (liquid-gas) injection. With little liquid remaining, and an angled thrust vector, parallel withdrawal would result in different depletion times and introduction of gases into the flow. Compensation would require additional components and accommodation would require additional weight. On the other hand, the center-of-gravity shift accompanying series expulsion is easily accounted for by an additional 0.5° angle TVC capability; this is a simple change with a Lockseal nozzle. Furthermore, the series expulsion would improve the thermodynamic survivability with F_2.

For pressurization, a pressure-regulated helium system was selected. In response to the mission thermodynamics with F_2, the He is stored at −310°F and is used at that temperature despite a small weight penalty. With ClF_5, the He is stored and used at the payload temperature. The pressure regulator represents one of the most critical dynamic control components in the system and was selected on the bases of accuracy, simplicity, compatibility with fluorinated

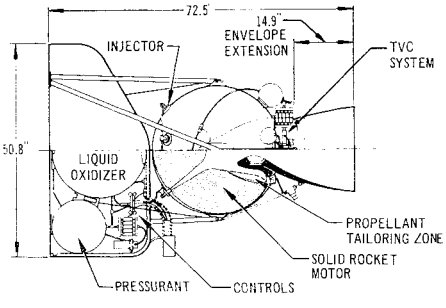

Fig. 6 ClF_5 engine for 2400-lb spacecraft.

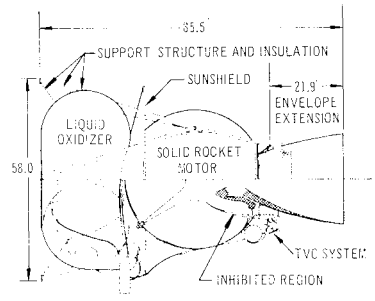

Fig. 7 F_2 engine for 5000-lb spacecraft.

compounds between −310°F and 70°F, insensitivity to environmental factors, very low gas leakage, and a well-proved design concept. A downstream-sensing, spring-biased bellows design suitably modified for the fluids in question was selected. The design was submitted by Pneumo-Dynamics Corp.

Explosive-actuated valves were selected after considering solenoid-operated valves, electrically-piloted hydraulic or pneumatically-actuated valves, and various types of explosive valves. Evaluation criteria included simplicity and reliability, compatibility with fluorinated liquid, zero leakage, action time ~10 msec, insensitivity to temperature, and well-characterized concept. A normally-closed design capable of two full cycles of operation was selected for helium isolation, liquid isolation and flow control, and TVC isolation functions. The design maintains tight, leak-free metal-to-metal interference fits for the half-cycle actuation strokes required. Five valves in parallel are used for each isolation valve bank, providing the required ten on-off cycles of operation. The design was submitted by the SieBelAir Corp.

Six aluminum multiorifice injectors are used on all motors. They are arranged and canted to provide the required spray pattern, within the annulus of the grain, using criteria developed from hybrid as well as fluid-controlled solid experience. "Chugging" stability criteria and atomization requirements were used to establish a minimum pressure drop across the injector of 25% of the combustion pressure or 100 psi, whichever was greater. Combustion instabilities are not encountered in combined liquid/solid motors.

Stainless steel tubing is used for all plumbing. Weld socket design is used to provide leak-tight hermetic seals. Several welding techniques may be considered to meet the high-integrity, low-porosity requirements. The one type of joint between dissimilar materials is located at the injectors, and vacuum-diffusion brazing with a transitional alloy at the interface can be considered to eliminate any leakage possibility. The injector manifold is wishbone shape to facilitate assembly. A filter is located upstream of the valves, and an orifice is placed in the lines upstream of the injectors as a simple emergency back-up feature.

Propulsion System Configuration and Structure

Propulsion system assemblies representative of the two propulsion sizes and liquids are presented in Figs. 6 and 7. Figure 6 is the design for the 2400-lb vehicle with ClF_5, and Fig. 7 is the design for the 5000-lb vehicle with F_2. As shown, optimal expansion ratios result in propulsion system lengths longer than those initially specified when tankage is packaged forward.

All fluid components that are a part of the oxidizer supply system are packaged inside a common insulation barrier. Thermal survivability of F_2 was shown to be predicated upon effective isolation from external radiative and internal conductive heating. Isolation from the payload, sun, and Mars is provided by a cocoon of "superinsulation" comprised of multiple layers of aluminized mylar separated by Dexiglas. Also, an insulated sunshield is located between the solid rocket motor and F_2 tanks. A portion of the LF_2 tankage perimeter is exposed to space to permit radiative cooling,

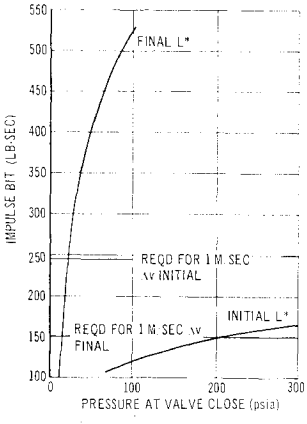

Fig. 8 Impulse bit variation with pressure at valve command close; pressure-feedback control mode, F_2 engine for 2400-lb spacecraft, 3-g thrust level.

provided the toroidal payload design can be changed to a forward location. Because the tank structural support system provides a source of potentially severe internal penetration heating, struts were replaced with a titanium tension wire support system (high ratio of strength-to-thermal diffusivity). ClF_5 engines are similarly insulated, except that a sunshield is not required where the payload is positioned forward. The insulation prevents freezing. With the toroidal payload, the ClF_5 is warmed by the payload and a sunshield is needed to prevent overheating by solar radiation.

Oxidizer and pressurant tanks for the small vehicle are tied together by doublet skirts. For the large vehicle, tanks are mounted in a perforated steel basket that proved lighter than a doublet skirt because of the greater number of tanks. With either system, six titanium tension wires are attached to provide the principal means of support.

The propulsion module is a totally integrated assembly that attaches to the payload; eight steel tubular supports in an "A-frame" array are attached to the solid rocket motor by pin-type hangers and to the payload pads by bolts.

Control Systems

The Lockseal TVC system consists of a movable nozzle actuated by two pressurized hydraulic cylinders at 90° to each other. Reinforced elastomeric elements allow the nozzle to be deflected by shear deformation of the elastomer. The element and adjacent metal reinforcements are surfaces of spherical sectors with center of rotation at the nozzle throat. The seal is adhesively bonded to the reinforcements on both sides. Combinations of push-pull allow omnidirectional vector positioning. Once positioned, the system requires no further power. The system consists of a hydraulic accumulator (elastomeric bladder expulsion), pressure regulator, valves, actuators, and oil sump. Linear position transducers generate control feedback signals. The hydraulic actuators are controlled by a four-way, two-position servovalve (Cadillac Gage Corp.), and oil is admitted to the pressure regulator through a bank of five SieBelAir valves serving isolation and control functions generically similar to the oxidizer system.

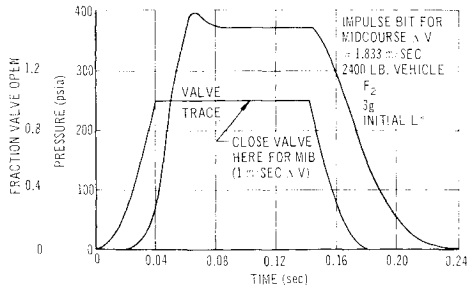

Fig. 9 Midcourse correction impulse bit trace.

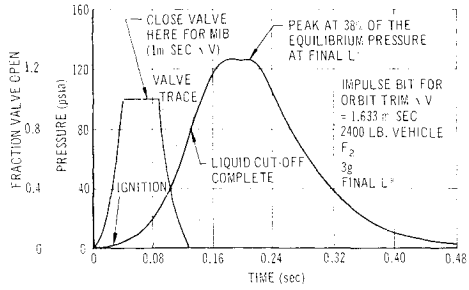

Fig. 10 Orbit trim impulse bit trace.

Minimum-impulse-bit capability was characterized by performing parametric transient ballistics calculations based on pressure-feedback control of valve command close. Following ignition, the valve is commanded to close at a certain pressure during pressure rise and the resulting impulse bit is determined. Results for the small F_2 engine, 3-g design, are typical and shown in Fig. 8 for initial and final L^* values. At initial L^*, a finite equilibrium duration will be permissible for the MIB because the completely transient mode produces smaller impulse bits. At final L^*, however, pressure-feedback control will have to be employed early in the pressure rise time; the consequence is reduced impulse bit accuracy. A design at 1-g thrust will have improved accuracy, and at 5-g the accuracy will not be as good. Effects of valve action time and profile were examined, and line fill and evacuation were taken into account.

Based on these results, midcourse correction impulse bits can be controlled by comparing a reference signal, indicative of the ΔV magnitude sought, with an integrating accelerometer signal accumulated during the impulse interval. The motor is shut down when the accumulated ΔV falls short of the specified ΔV by the predicted tail-off imposed ΔV. A representative midcourse correction impulse bit is shown in Fig. 9. Larger impulse bits, including the long orbit insertion burn, are also controlled by this technique and will be more accurate as the transient portions assume less significance. The orbit insertion burn tail-off must be based on the larger L^* which follows the depletion of the bulk of the solid propellant in that single burn.

Orbit-trim, minimum-impulse burns retain the pressure-feedback control mode because of the requirement for a completely transient pulse at high L^*. It is more accurate to control from the precharacterized interior ballistics than from the exterior ballistics in this mode. A pressure signal from the rocket motor is compared to a telemetered signal level indicative of the pressure required at shutdown to deliver the specified ΔV. A representative orbit trim impulse bit is shown in Fig. 10. For orbit trim ΔV requirements in excess of about 15m/sec, the control then can be switched over to the integrating accelerometer channel for improved accuracy and finite equilibrium operation.

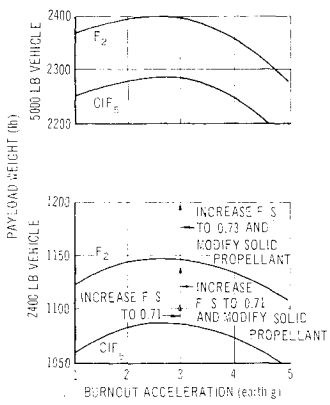

Fig. 11 Variation of payload capability.

Impulse-bit error analysis was performed to establish MIB accuracy. Influence coefficients were obtained for all potential error sources, and errors were assigned to these sources. Batch-to-batch variability in the pressure exponent of the solid propellant burning rate was the major potential error source. Nevertheless, MIB accuracy was within specifications at thrust levels below 5-g. At 5-g, a throttling system may be necessary for MIB thrusting.

Control system circuits and command logic are selected to minimize electrical power requirement.[3] Current requirements can be limited to 5 amp at 12 or 24v by sequential firing of the explosive valves. Only 3 w-sec of energy are required to fire all valves. The TVC servovalves require 8 ma each at full flow. It was assumed that these requirements could be satisfied by the payload power supply.

All fluid tanks contain the provision for ground and flight monitoring of system condition with skin-patch thermocouples and pressure and pressure transducers. Unlike the ClF_5 systems, the LF_2 systems have a thermal maintenance requirement. Subcooled LN_2 is used in conjunction with external heat exchangers to cool the helium and oxidizer tanks before filling. This system also maintains the oxidizer several degrees below its normal boiling point before launch. A low-pressure, dry N_2 purge flowing through the superinsulation is used to prevent condensation of atmospheric moisture within the insulation before launch.

The designs provide for remote fill and emergency drain operations. Helium is loaded first and may be approached for a leak inspection of the system (man-rated safety factor). Once oxidizer loading begins, all operations and checkout are remote. The system may then be approached only after emergency drain procedures are complete and the system essentially disarmed.

A first motion umbilical disconnect unit severs the system from ground-controlled disarm functions, heat exchanger and nitrogen purge, and the system is committed to flight.

Results

Payload capability vs design acceleration level for each of the four propulsion systems is shown in Fig. 11. These curves were generated from detailed performance and weight analyses, which established that the detailed designs provided a total ΔV in excess of the mission requirement by 7%. A final size iteration established the payload capability at the specified ΔV, as shown. The optimum acceleration level is ~ 3 g, above which pressure-sensitive weights increase rapidly and below which burn-time sensitive weights increase.

Payload growth potential by operating at a higher F/S and modifying the solid propellant is also included in Fig. 11 for the 2400-lb vehicle. These changes in the ClF_5 system are nearly as effective as replacing ClF_5 with F_2 and would likely be more cost-effective and permit greater mission and design flexibilities. The full potential through continued solid-propellant advances is not projected but is likely to be considerable.

The only potential failure mode unique to the fluid-controlled solid is solid-propellant extinguishability. Other failure modes would also appear in a conventional solid rocket and in that part of an inert gas-pressurized liquid rocket associated with the delivery of only one of the two liquids.

A detailed development program plan was constructed that includes all critical problem/characterization areas defined in this study. Some of the more important areas include solid propellant extinguishability following long burn times, nozzle erosion in the course of long burn times, impulse bit characteristics, full-scale delivered performance over a range of F/S, more detailed and refined mission thermodynamics analysis (including better characterization of Mars heating) and those aspects of state-of-the-art technology not as yet fully reduced to flight practice (chiefly involving fluorinated liquid). The program plan spans a 3-yr period through (pre-flight rating test).

Conclusions

The fluid-controlled solid rocket motor can perform the intended NASA mission. Liquid fluorine is preferred over OF_2 as an advanced liquid injectant for this particular application. However, use of either cryogen with the toroidal payload configuration associated with the large vehicle is thermally infeasible. Additional study is required. The propulsion system has been defined and optimized for each of two sizes and ClF_5 and F_2 liquids. A basis for development and areas of growth potential have been defined.

References

[1] Bonin, J. H., Coates, R. L., and Cohen, N. S., "Thrust Magnitude and Restart Control of Solid Motors by Injection of Hypergolic Fluids," *Journal of Spacecraft and Rockets*, Vol. 4, No. 3, March 1967, pp. 354–358.

[2] Hough, R. W. and Meitner, J. G., "Continued Investigation of Solid Propulsion Economics, Task 4, Cost Projections for New Sounding Rockets and Upper Stages," Contract NAS 7-309, Menlo Park, Calif. Sept. 1967, Stanford Research Institute.

[3] Cohen, N. S. and Small, K. R. "Study and Development of a Fluid-Controlled Solid Rocket Motor for Space Application," Rept. LPC-929F, Vols. I and II, Contract NAS 7-701, Feb. 1969, Lockheed Propulsion Co., Redlands, Calif.

[4] Cohen, N. S., Price, C. F., Coates, R. L. and Small, K. R., "Characteristics of Fluid-Controlled Solid Rocket Motors for Space Applications," *Proceedings of the 3rd ICRPG/AIAA Solid Propulsion Conference*, Chemical Propulsion Information Agency Publication 167, Vol. I, 1968, pp. 319–340.